

3D Face Recognition using Kinect

Rahul Ajmera

Department of Computer
Science and Engineering,
Indian Institute of Technology
Kanpur, India
rahulaaj@cse.iitk.ac.in

Aditya Nigam

School of Computing and
Electrical Engineering,
Indian Institute of Technology
Mandi, India
aditya@iitmadi.ac.in

Phalguni Gupta

Department of Computer
Science and Engineering,
Indian Institute of Technology
Kanpur, India
pg@cse.iitk.ac.in

ABSTRACT

2D Face recognition systems bound to fail on images with varying pose angles and occlusions. Many pose invariant methods are proposed in recent years but they are still not able to achieve very good accuracies. So in order to achieve a better accuracy we need to extend algorithms over 3D faces. Due to the high cost involved in acquisition of 3D faces we developed our approach for low-cost and low-quality Microsoft Kinect Sensor and propose an algorithm to produce better results than existing 2D Face recognition techniques even after compromising on the quality of the images from the sensor. Our proposed algorithm is based on modified SURF descriptors on RGB images combined with various enhancements on automatically generated training images using Depth and Color images. We compare our results obtained with State Of The Art Techniques obtained on publicly available RGB-D Face databases. Our System obtained recognition rate of 98.07% on 30° CurtinFace Database, 89.28% on EURECOM Database, 98.00% on 15° Internal Database and 81.00% on 30° Internal Database.

Keywords

Microsoft Kinect, Face Recognition

1. INTRODUCTION

Face is the most easily obtainable and convenient trait which is the least objectionable to the users and is one of the most popular biometric traits used currently for recognition and verification security systems. But there are many challenges in face based human recognition systems with pose, lighting intensity, occlusion, age and facial expressions as the major factors. 3D Face recognition system extends in solving the problem of occlusion, pose invariance and illumination variation in 2D face recognition systems. In real life, identification systems are needed for non-cooperative individuals hence the system should be robust to pose and occlusions. Since most of the security systems want their system to work with face images at arbitrary angle, 3D data

Permission to make digital or hard copies of all or part of this work for personal or classroom use is granted without fee provided that copies are not made or distributed for profit or commercial advantage and that copies bear this notice and the full citation on the first page. Copyrights for component of this work owned by others than ACM must be honored. Abstracting with credit is permitted. To copy otherwise, or republish, to post on servers or to redistribute to lists, requires prior specific permission and/or a fee. Request permissions from Permissions@acm.org.

ICVGIP '14, December 14-18, 2014, Bangalore, India
<http://dx.doi.org/10.1145/2683483.2683559>

helps in improving the recognition rate for such systems. But, there is very less work done on it especially because of expensive 3D sensors and high computation time.

Eyes and nose features are extracted from 3D model using Gaussian Curvature based landmark points and is proposed in [11]. [12] describes representation of global curvature in the form of Extended Gaussian image accompanied by MCPMFC classifier. EGI, a histogram like feature vector is used for feature extraction. The first 3D morphable face model using 2D images was proposed in [13]. Optical Flow based correspondence is used to create 3D model. ASM model is trained on 2D images to mark landmark points to create a 3D template model based on stereo images in [14]. A new template CANDIDE-3 model created by nose, eyes and mouth landmark points is proposed in [15]. Automatic facial features are extracted using information from frontal and profile face. A LBP fused with covariance descriptor are used for feature extraction in [5]. 2D images of face at different poses from 5° to 90° are automatically created using 0° RGB and Depth images. [7] describes a sparse coding based similarity fusion on RGB and Depth images with pose correction and symmetric filling. Pose correction based on reference model is followed by symmetric filling on left and right side. A fused similarity score is obtained by applying sparse coding on depth map and color image independently. HOG based approach on RGB entropy, Depth Entropy and Visual Saliency Map used as features with Random Decision Forest Classifier is described in [4]. A 3D Depth and Intensity based on Gabor Filter using Adaboost classifier and symbolic PCA to decrease time complexity is proposed in [9]. 3D Radon transformation is applied before extraction of features using Gabor wavelets.

Now with launch of Kinect Camera for software development by Microsoft in 2011, the problem of cost and high computation time is solved with a compromise on the quality of images because both RGB and Depth images are of size 640×480 pixels. As a result we have advantage of using 3D features of face for feature extraction but disadvantage over the quality of image as compared to high resolution 2D camera. This paper proposes a method of human recognition using low quality Kinect Sensor images with gallery image creation using graph based interpolation and surf based feature extraction and matching on enhanced images.

2. PROPOSED APPROACH

This section explains step by step the complete process of human identification using Kinect RGB+Depth data. Unregistered Kinect RGB and Depth data is registered using

Fakenect tool. Face from the input data is cropped using Viola Jones. In the pre-processing stage, background is removed, noisy depth image is enhanced using Median Filter, training images are created using Automatic Nose-Tip Detection and Graph Based Iterative Hole Filling Interpolation. Intensity images are enhanced using Adaptive Histogram Equalization, Non Local Means Filter and Steerable Filter and features are extracted in all 3 enhanced images independently using SURF. Finally a weighted score fusion is done on similarity scores and identity of test image is reported.

2.1 Registering Kinect RGB and Depth Images

Kinect gives unregistered RGB and Depth images. It uses different cameras for capturing RGB and Depth data. Hence we used OpenKinect tool fakenect to capture and register RGB and Depth image which uses Kinect camera's intrinsic and extrinsic properties with corner based calibration. An example of registered depth image is shown in Figure 1 .

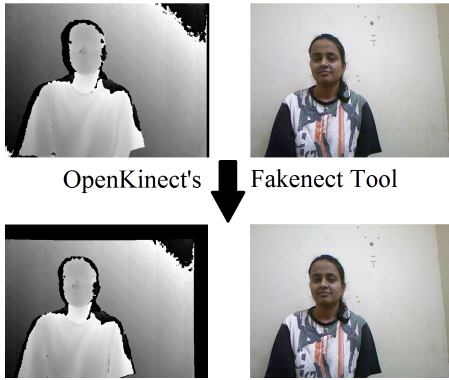


Figure 1: Registered Depth Image using Fakenect

2.2 Face Cropping

Viola Jones Face Detection [3] works well for frontal and profile faces but for other pose angles they fail to crop the face automatically. Hence in order to continue with our algorithm all faces are cropped manually. For tackling the scale problem all faces are resized to 100×100 to maintain uniformity. The registered depth image is cropped automatically using the same coordinates as of RGB image.

2.3 Pre-Processing

This section describes all the enhancements, filters and training images creation required before feature extraction.

2.3.1 Background Removal

Background may contribute in key point extraction hence it is required to remove it. On the assumption that background pixels are whiter than the foreground and have large depth values as compared to face pixels, empirically thresholds for both intensity and depth are used to remove the background, Figure 2 shows an example of background subtraction.

2.3.2 Enhance Depth

Kinect Depth images are very noisy hence denoising is required. Also registration process may add noises to the



Figure 2: Background removal based on depth and intensity Thresholds

image. Since we don't want any loss of information, median filter is used to remove noises and fill in gaps. An example of application of median filter on RGB and depth Image from Internal database is shown in Figure 3.

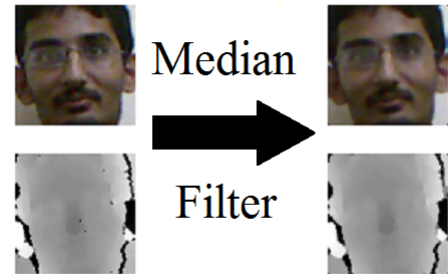


Figure 3: Median Filter Enhanced Images

2.3.3 Automatic Nose-Tip Detection

The proposed algorithm is an iterative process of reducing the nose-tip candidates in the cropped image at every stage of the process. The algorithm is basically divided into 4 stages and is applied on Depth images:

- **Highest Intensity** First of all, the face depth image as shown in Figure 5(a) is analyzed and all the pixels having intensity (energy) greater than all it's 3×3 neighboring pixels are shortlisted as the nose-tip candidates as shown in Figure 5(b).
- **Thresholding** Two types of thresholding, one on the intensity of the pixel and other on the variance of the pixel are used. Threshold over intensity is used to be 90% of all the intensity values in the image, i.e. nose-tip should be among the top 10% intensity values in the Depth image as shown in Figure 5(c). Secondly, we came with an optimal threshold value of 400 on variance from the assumption that neighboring pixels will have similar intensities as shown in Figure 5(d).
- **Nose-Area** Now, we may still be left with many candidates on the cheeks and the forehead, so we consider the nose to lie in the rectangle with dimensions $(0.25x, 0.50y), (0.75x, 0.69y)$ with face dimensions from [8] as shown in Figure 4 .
- **Nose-Tip** Finally, we select the centroid of the pixels with highest intensity in the nose-area as our nose-tip as shown in Figure 5(f).

The complete process is explained with an example in Figure 5 .

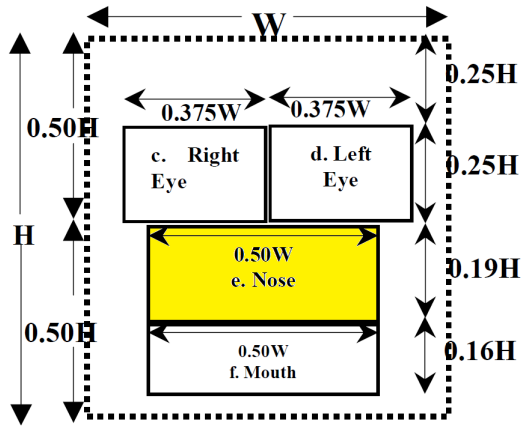


Figure 4: Geometric Division of Frontal Face [8]

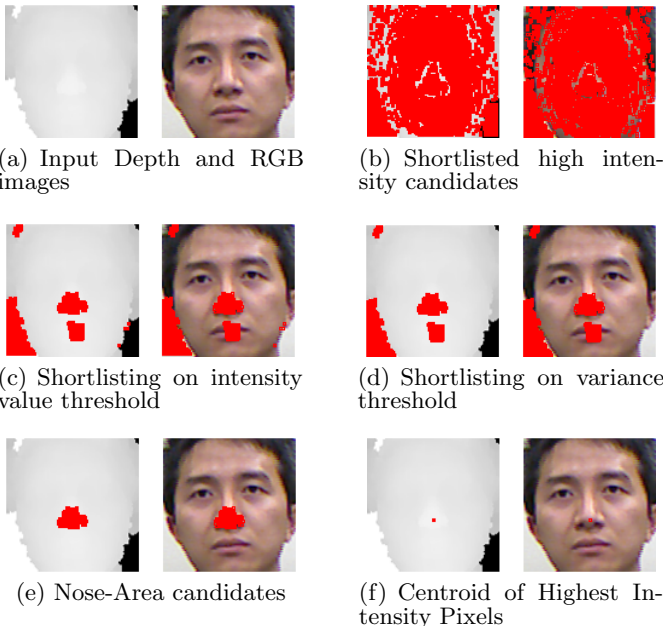


Figure 5: Step by step process of Automatic Nose-Tip Detection

2.3.4 Create Gallery Images

This is the crucial part of the algorithm. 18 gallery images with pose angles $0^\circ, 5^\circ, 10^\circ, 15^\circ, 20^\circ, 25^\circ, 30^\circ, 35^\circ, 40^\circ, 45^\circ, 50^\circ, 55^\circ, 60^\circ, 65^\circ, 70^\circ, 75^\circ, 80^\circ, 85^\circ$ and 90° are created as shown in Figure 6 using 0° Depth and RGB images.



Figure 6: Expected 18 Gallery Images

The complete Algorithm is described below:

- Color image(0°), Depth image(0°) and pose angle are taken as input.
- Automatic Nose-Tip detection as described in previous subsection is used to detect nose-tip.
- An XYZ matrix from RGB and Depth image is created and the matrix is rotated about y-axis passing through Nose-Tip using the transformation matrix in Equation 1

$$R = \begin{bmatrix} 1 & 0 & 0 \\ 0 & \cos \theta & -\sin \theta \\ 0 & \sin \theta & \cos \theta \end{bmatrix}. \quad (1)$$

- The rotated matrix is rounded off to nearest integers and color of pixels are taken from input RGB image and pixels with no correspondence in original image are given 0 (Black) value.
- Noises generated after rotation are removed using 3×3 filter with a threshold on number of black neighbor pixels.
- A graph based iterative hole filling interpolation is used to fill in black pixels. All black pixels who have some non-black neighbors greater than a threshold are filled iteratively. Using a 3×3 filter in the 1st iteration some pixels having non-black neighbors are filled with their average value reducing the number of black pixels for next iteration. In next iteration same process is repeated and some more pixels are filled with non-zero intensity values. This process is stopped after n iterations. Experimentally n is found to be working well for value 5.
- After interpolation, three median filters of size 3×3 are applied on R, G and B images separately to remove the remaining noises.

A complete flow of steps for gallery image creation using an example is shown in Figure 7 . For every subject 18 images are created which are used as gallery images and captured pose angle images as the testing images.

2.4 Enhance RGB

Three types of enhancement are applied on RGB images to remove noises produced due to rotation or Kinect data capturing. Adaptive Histogram Equalization (enhance low

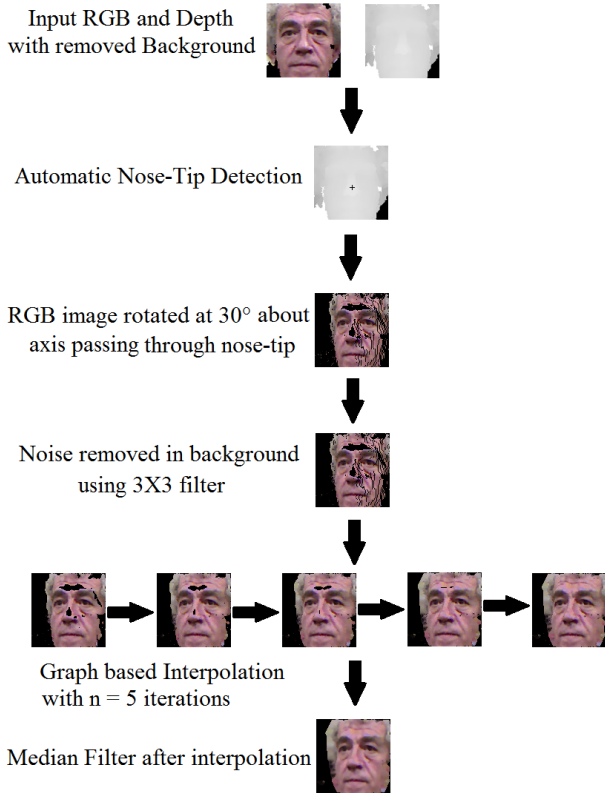


Figure 7: Work Flow of 30° gallery image creation

contrast), Non Local Means Filter (removal of pepper noise) and Steerable Filter (illumination invariance) are applied separately on greyscale images (SURF uses only greyscale images) and are used for feature extraction.

2.4.1 Adaptive Histogram Equalization

Histogram equalization is one of the most common contrast improving image processing technique in literature. The cumulative distribution function of probability of occurrence of pixel with value i is given by $p(i) = n_i/n$ where n_i is number of pixels with value i and n is the total number of pixels transformed using Equation 2 .

$$cdf'(x) = cdf(x) \left[\max_y \{ cdf(y) \} - \min_y \{ cdf(y) \} \right] + \min_y \{ cdf(y) \} \quad (2)$$

Adaptive histogram equalization is a variation of histogram equalization. The complete image are divided into $a \times b$ small windows of equal size and histogram equalization as described earlier is applied over each window. After combining all the windows a bilinear filter is used at the boundaries to uniformize the transition. An example of Adaptive Histogram Equalization over a face from CurtinFace database is shown in Figure 8.

2.4.2 NLM filter

Non-Local Means is a very popular filter to denoise noisy images. The basic assumption of this technique is that every natural image contains self-similarity. Most denoising filters consider neighborhood to assign new value to the pixel, but as it's names suggest, it finds similar pixels in the image and

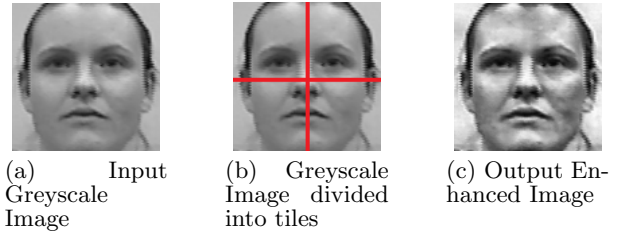


Figure 8: Adaptive Histogram Equalization Enhanced Image

use them to obtain value of the pixel. Similarity function between two pixels is defined as in Equation 3 where P_i and P_j are patches at pixels i and j respectively.

$$S(i, j) = \frac{\|P_i - P_j\|}{n^2} \quad (3)$$

$W_{ij} = e^{\frac{S(i,j)}{2\sigma^2}}$ is the weight provided to the j^{th} pixel. The weights are normalized and are multiplied with intensity values of similar pixels to obtain new intensity value of i^{th} pixel as shown in Equation 4 where \hat{W}_{ij} is the normalized W_{ij} .

$$I'(i) = \sum_j \hat{W}_{ij} * I(j) \quad (4)$$

Figure 9 shows an example of NLM denoising over face images from CurtinFace database.

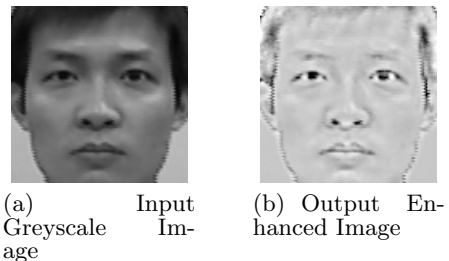


Figure 9: Non-Local Means Filter Enhanced Image

2.4.3 Steerable Filter

Sometimes multiple filters of different orientations are needed to remove all type of noises. Steerable Filter provides a way to create a linear combination of basic filters each with different orientation. For example consider a Gaussian filter given by Equation 5

$$G(x, y) = e^{-(x^2+y^2)} \quad (5)$$

A steerable filter in two dimensions can be created as in Equation 6.

$$SF^\theta = \cos \theta * \frac{\partial G}{\partial x} + \sin \theta * \frac{\partial G}{\partial y}$$

or

$$SF^\theta = \cos \theta * (-2xe^{-(x^2+y^2)}) + \sin \theta * (-2ye^{-(x^2+y^2)}) \quad (6)$$

A weighted combination of multiple SF^θ 's can be used to enhance noisy Kinect Images. In our case we use 8 different

equally spaced angle filters from 0° to 360° and Figure 10 shows denoising of face image from CurtinFace database by application of average of all 8 Steerable Filters.

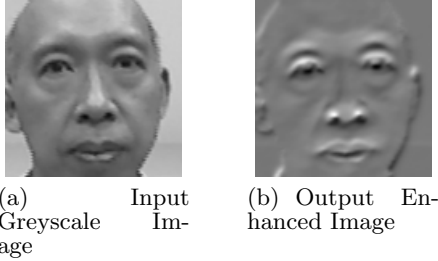


Figure 10: Steerable Filter Enhanced Image

2.5 Feature Extraction & Matching

SURF is used for feature extraction on all 3 enhanced images. SURF features are very distinctive, invariant to scale and rotation and fast to calculate. Each key point is described using 64-bit vectors. Features for both training and testing images are extracted for all 3 enhancements separately and kept in the database.

2.5.1 Key Point Detection

Key point detection is based on Hessian Matrix. For a point $X = (x, y)$ in a image, $H(X, s)$ is defined as in Equation 7 for a given scale s .

$$H(X, s) = \begin{bmatrix} L_{xx}(X, s) & L_{xy}(X, s) \\ L_{yx}(X, s) & L_{yy}(X, s) \end{bmatrix}. \quad (7)$$

where Laplacians are defined as in Equation 8 and g is Gaussian Function.

$$L_{ab}(X, s) = \frac{\partial^2 g(s)}{\partial a \partial b} \quad (8)$$

$\arg \operatorname{localmax}(\det(H(X, s)))$ gives the interest or key points. For speeding up the calculations, determinant calculation is done by integer approximation using integral images.

2.5.2 Key Point Description and Matching

For making the descriptor rotation invariant a direction is required which is invariant to it. Integral images are used to calculate Haar Wavelet responses in x and y directions. After calculating the responses, the dominant response is used to estimate the orientation of key point, A square region oriented along the dominate response vector with center at the key point is considered. The square region is divided into 4×4 smaller windows and a feature descriptor of each window is calculated as in Equation 9

$$v = \left[\sum h_x, \sum h_y, \sum |h_x|, \sum |h_y| \right] \quad (9)$$

Where h_x and h_y are haar wavelet responses in x and y direction respectively. So, the complete key point descriptor is obtained by joining vectors for all windows making the descriptor of length $4 \times (4 \times 4) = 64$.

Matching of 2 key point sets from different images is important and is done based on nearest neighbor matching. An example of SURF based Key Point Matching between two images of Internal database is shown in Figure 11 .



Figure 11: Matched SURF Key Points on different pose images

2.6 Score Fusion

SURF based feature extraction and matching is done for all 3 enhancements independently. A final matching score is obtained by empirically weighing the scores as shown in Equation 10 where w are weights and s are similarity scores.

$$s_{final} = \frac{w_{ahe} * s_{ahe} + w_{nlm} * s_{nlm} + w_{sf} * s_{sf}}{w_{ahe} + w_{nlm} + w_{sf}} \quad (10)$$

After obtaining the final matching similarity score, the identity of test image is given by identity of training image with maximum similarity score among all training images. The complete work-flow of proposed approach is shown in Figure 12.

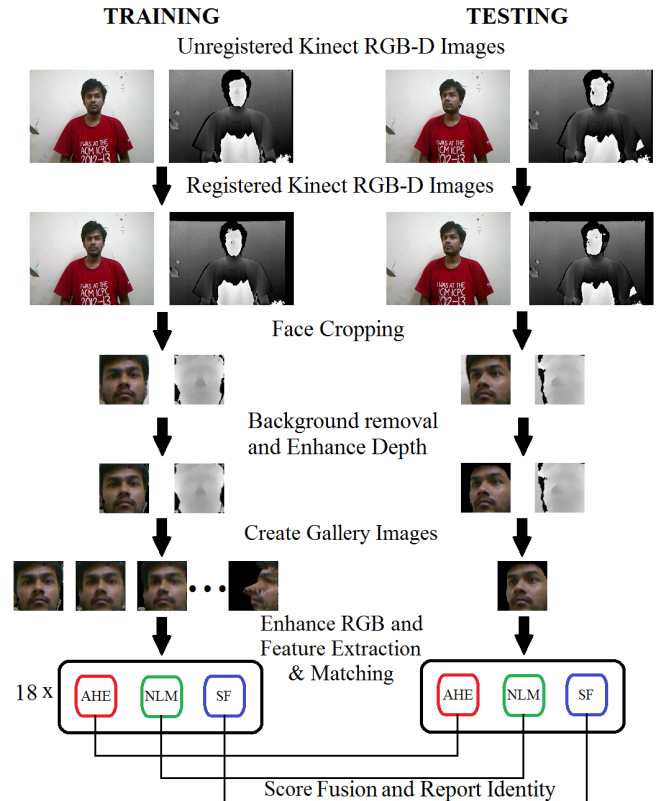


Figure 12: Work Flow of Proposed Approach

3. EXPERIMENTAL RESULTS

3.1 Databases

Two public databases EURECOM and CurtinFace and one Internal database are used to analyze the performance of proposed approach. Table 1 shows summary of the 3 databases.

EURECOM [1] Database consists of 52 subjects (14 females, 38 males). The data is collected in two sessions with a gap of about half month. In each session 9 images per subject are taken with left profile face, high illumination face, neutral face, occlusion with sunglasses face, occlusion with hand face, occlusion with paper face, mouth open face, smiling face and right profile face representing the 9 images in order. An example of one session images of a subject are shown in Figure 13 .

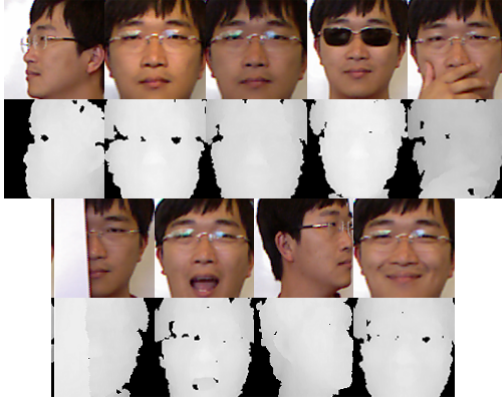


Figure 13: Single Session RGB + Depth images of EURECOM Database

CurtinFace [2] Database consists of 52 subjects with mix of males/females and with/without spectacles. There are 7 images per subject at 0° , $\pm 30^\circ$, $\pm 60^\circ$, $\pm 90^\circ$ pose angles. Some subjects show large illumination variation in frontal and other pose angle images. An example of different pose angle images of a subject are shown in Figure 14 .

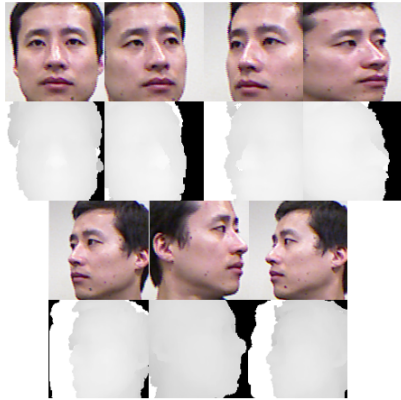


Figure 14: Single Session RGB + Depth images of CurtinFace Database

Internal Database consists of 100 subjects with mix of males/females and with/without spectacles. There are 7

images per subject at 0° , 15° , 30° , 45° , 60° , 75° , 90° pose angles. Some subjects show illumination variation in frontal and other pose angle images. Figure 15 shows an example of different pose images of a subject.

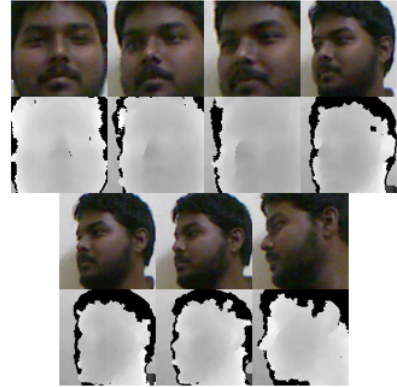


Figure 15: Single Session RGB + Depth images of Internal Database

3.2 Testing Strategy

Two testing strategies based on previous papers are used to compare performance of the system. Table 2 shows the experimental weights used for different enhancements techniques for different databases. Since, the gallery images created in CurtinFace and Internal databases are very noisy and also have large illumination variations as a result large weights are provided for Non-Local Means Filter (for noise) and Steerable Filter (for illumination) .

3.2.1 Test Protocol A

Five fold random sub-sampling based testing on rank-1 accuracy. For example in case of EURECOM database with 18 images per subjects, randomly 4 images ($round(18/5)$) are used for training and 14 images ($18 - round(18/5)$) for testing. This experiment is repeated for 100 iterations and average rank-1 accuracy is reported.

3.2.2 Test Protocol B

18 Gallery images as described in Proposed Approach section, created using 0° RGB and Depth images are used as training images and captured different pose images as the testing images.

3.3 Comparison with Previous Approach

3.3.1 EURECOM Database

Test Protocol A is used to compare with previously existing technique. Our technique obtained 89.28% average CRR. Table 3 compares results on CRR.

3.3.2 CurtinFace Database for 30° pose images

Test Protocol B is used to compare with previously existing technique. Our technique obtained 98.07% CRR . Table 4 compares the results based on average CRR.

3.4 Results on Internal database

3.4.1 Test Protocol A

Our technique obtained 89.26% average CRR.

Table 1: Overview of Databases

Database	Subjects	Images	Remarks
EURECOM	52	$52(\text{subjects}) \times 9(\text{poses}) \times 2(\text{sessions}) = 936$	Occlusion and variation in pose and expression
CurtinFace	52	$52(\text{subjects}) \times 7(\text{poses}) = 364$	Pose and illumination variation in some subjects
Internal	100	$100(\text{subjects}) \times 7(\text{poses}) = 700$	Pose and illumination variation in some subjects

Table 2: Empirical weights for different enhancements

Database	Adaptive Histogram Equalization (AHE)	Non-Local Means Filter (NLM)	Steerable Filter (SF)
EURECOM	0.33	0.33	0.33
CurtinFace	0.26	0.37	0.37
Internal	0.20	0.40	0.40

Table 3: Testing Protocol A based Average CRR comparison on EURECOM Database

Approach	CRR
Proposed Approach w/o enhancements	76.13%
HOG + Entropy + Saliency [4]	88.50%
Proposed Approach	89.28%

Table 4: Testing Protocol B based CRR comparison on CurtinFace Database for 30° images

Approach	CRR
Proposed Approach w/o enhancements	82.69%
LBP + Covariance Descriptor [5]	94.23%
Proposed Approach	98.07%

3.4.2 Test Protocol B for 15° pose images

Our technique obtained 98.00% CRR.

3.4.3 Internal Database for 30° pose images

Our technique obtained 81.00% CRR, which was 64.00% without the 3 enhancements.

CMC curve for Test Protocol A and Test Protocol B are shown in Figure 16(a) and Figure 16(b) respectively.

3.5 Time Complexity

Creation of 18 gallery images is a one-time process, hence excluding it from computing complexity on an average identification takes 1.35 sec for internal database of 100 subjects, 0.47 sec for EURECOM database of 52 subjects and 0.43 sec for CurtinFace database of 52 subjects. Also, on an average 0.31 sec are required to generate 18 gallery images for each subject.

4. CONCLUSION

A Kinect based 3D Face Recognition system is proposed in this paper. After registration of Kinect RGB and Depth data, manual cropping of face is done. After resizing all the images to same size, gallery images are generated automatically using graph based interpolation with some pre-processing on RGB and Depth data. SURF with Adaptive Histogram Equalization, NLM Filter and Steerable Filter are used for feature extraction and matching is done using

nearest neighbor key points. Average CRR of 89.28% are obtained for EURECOM database. Results in CurtinFace database are found to be 98.07% CRR for 30° test images which failed on subject with very less illumination in frontal image. Internal database using the testing strategy of EURECOM database obtained 89.26% CRR . Internal database using test strategy of CurtinFace obtained 98.00% CRR on 15° test images and 81.00% CRR on 30° test images . The results obtained for public databases are better as compared to the state-of-the-art techniques. Some of the failed cases from different databases are shown in Figure 17 with along with explanation for failing of proposed approach.

5. REFERENCES

- [1] Tri Huynh, Rui Min, and Jean-Luc Dugelay. "An Efficient LBP-based Descriptor for Facial Depth Images applied to Gender Recognition using RGB-D Face Data." In ACCV Workshop on Computer Vision with Local Binary Pattern Variants, Daejeon, Korea, November 2012.
- [2] Wan-Quan Liu, "CurtinFace Database", Department of Computing, 2011.
- [3] Viola, Paul, and Michael J. Jones. "Robust real-time face detection." In International journal of computer vision 57, no. 2: 137-154, 2004.
- [4] Goswami, Gaurav, Samarth Bharadwaj, Mayank Vatsa, and Richa Singh. "On RGB-D face recognition using Kinect." In Biometrics: Theory, Applications and Systems (BTAS), IEEE Sixth International Conference on, pp. 1-6, 2013.
- [5] Ciacco, Cesare, Lingyun Wen, and Guodong Guo. "Face recognition robust to head pose changes based on the RGB-D sensor." In Biometrics: Theory, Applications and Systems (BTAS), IEEE Sixth International Conference on, pp. 1-6, 2013.
- [6] Bay, Herbert, Tinne Tuytelaars, and Luc Van Gool. "Surf: Speeded up robust features." In Computer Vision ECCV, pp. 404-417, Springer Berlin Heidelberg, 2006.
- [7] Li, Billy YL, Ajmal S. Mian, Wanquan Liu, and Aneesh Krishna. "Using kinect for face recognition under varying poses, expressions, illumination and disguise." In Applications of Computer Vision (WACV), IEEE Workshop on pp. 186-192, 2013.
- [8] Paul, Sushil Kumar, Mohammad Shorif Uddin, and Saida Bouakaz. "Extraction of facial feature points

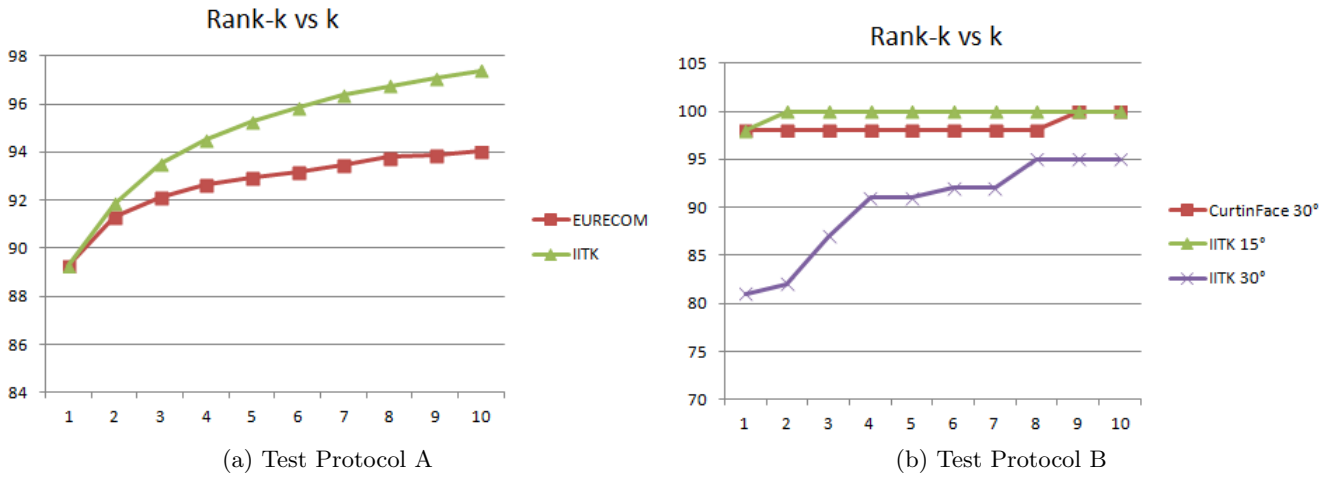


Figure 16: CMC Curves



Figure 17: Failed cases for various databases

- using Cumulative Histogram.” preprint:1203.3270, 2012.
- [9] PS Hiremath, PS Hiremath, and Manjunatha Hiremath Manjunatha Hiremath. ”3D Face Recognition Based on Depth and Intensity Gabor Features using Symbolic PCA and AdaBoost.” In International Journal of Signal Processing, Image Processing and Pattern Recognition 6, no. 5: 1-12, 2013.
- [10] Freeman, William T., and Edward H. Adelson. ”The design and use of steerable filters.” In IEEE Transactions on Pattern analysis and machine intelligence 13, no. 9: 891-906, 1991.
- [11] Suikerbuik, Rob, Hans Tangelder, Hein Daanen, and Aernout Oudenhuijzen. ”Automatic feature detection in 3D human body scans.” In No. 2004-01-2193. SAE Technical Paper, 2004.
- [12] Wong, Hau-San, Kent KT Cheung, and Horace HS Ip. ”3D head model classification by evolutionary optimization of the Extended Gaussian Image representation.” In Pattern Recognition 37, no. 12: 2307-2322, 2004.
- [13] Blanz, Volker, Sami Romdhani, and Thomas Vetter. ”Face identification across different poses and illuminations with a 3d morphable model.” In Automatic Face and Gesture Recognition, Fifth IEEE International Conference, pp. 192-197, 2002.
- [14] Naftal, A. J., Z. Mao, and M. J. Trenouth. ”Stereo-assisted landmark detection for the analysis of 3D facial shape changes.” In Technical report
- Department of Computation, UMIST, 2002.
- [15] Ansari, A-N., and Mohamed Abdel-Mottaleb. ”3D face modeling using two views and a generic face model with application to 3D face recognition.” In Advanced Video and Signal Based Surveillance, IEEE Conference, pp. 37-44, 2003.